AFM + Raman Microscopy + SNOM + Tip-Enhanced Raman: Instrumentation and Applications

P. Dorozhkin,* E. Kuznetsov, A. Schokin, S. Timofeev, and V. Bykov
NT-MDT Co., Build. 100, Zelenograd Moscow, 124482 Russia
* dorozhkin@ntmdt.com

Introduction

Atomic Force Microscopy (AFM) [1] has developed into a very powerful tool for characterization of surfaces and nanoscale objects. Many physical properties of an object can be studied by AFM with nanometer-scale resolution. Local stiffness, elasticity, conductivity, capacitance, magnetization, surface potential and work function, friction, piezo response—these and many other physical properties can be studied with over 30 AFM modes [1]. What is typically lacking in information provided by AFM studies is the chemical composition of the sample and information about its crystal structure. To obtain this information other characterization techniques are required, such as Raman and fluorescence microscopy. The Raman effect (inelastic light scattering) [2] provides extensive information about sample chemical composition, quality of crystal structure, crystal orientation, presence of impurities and defects, and so on. Information provided by Raman and fluorescence spectroscopy is complementary to the information obtained by AFM. So it is a natural requirement in many research fields to integrate these techniques in one piece of equipment—to provide comprehensive physical, chemical, and structural characterization of the same object. Of course, for routine studies of various samples, it is important to be able to obtain AFM and Raman/fluorescence images of exactly the same sample area, preferably with the same sample scan.

Instrumentation

Figure 1 shows typical setups integrating AFM with Raman/fluorescence microscopy (produced by NT-MDT Co.). The main technical requirement for such integration is positioning the high-resolution objective lens near the AFM cantilever without compromising AFM performance. The resolution, or numerical aperture (NA), of such an objective is one of the most important factors because it determines spatial resolution of the Raman/fluorescence maps as well as the sensitivity of the technique. Additionally, a tightly focused laser spot and the AFM probe must be spatially correlated with high precision and temporal stability to provide AFM and spectroscopy measurements from exactly the same sample area.

Two main geometries for AFM integration with high-resolution microscopy and spectroscopy are "upright" and "inverted," named for corresponding light microscopes (Figures 1a and 1b). The inverted configuration has the advantage of having the cantilever and laser spot coming from different sides of the sample. This eliminates effects of laser beam shadowing by the cantilever. Also, the inverted configuration allows the use of oil immersion optics (the oil is applied from the bottom of the sample and does not interfere with AFM) to deliver the highest possible light sensitivity and spatial resolution. The limitation of the inverted configuration is obvious: if simultaneous AFM and

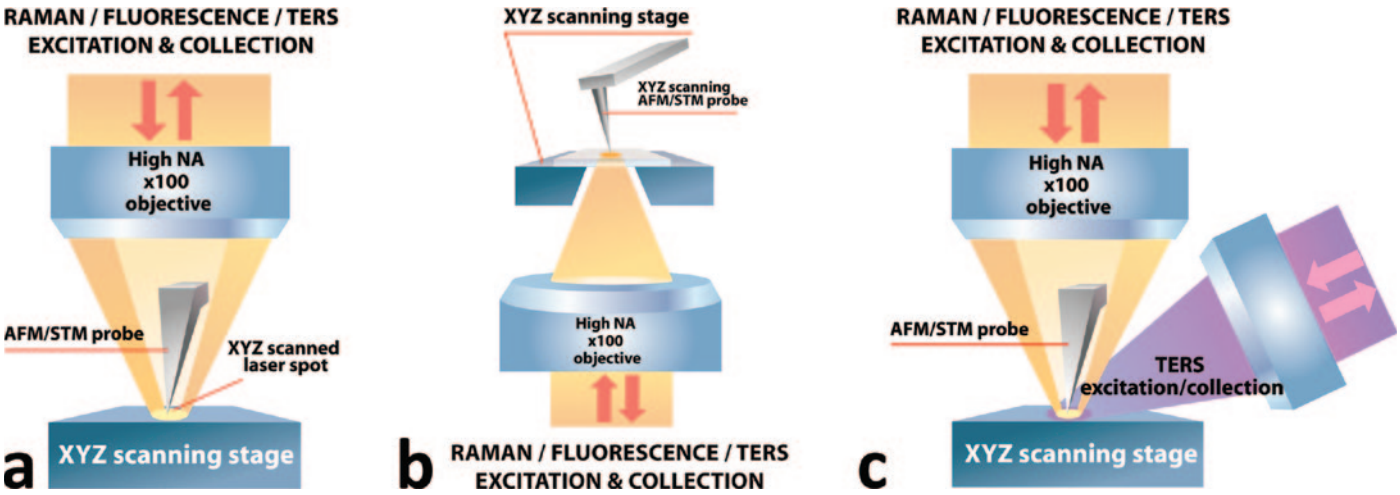

Figure 1: Typical experimental setups offered by NT-MDT Co. integrating Atomic Force Microscopy with confocal Raman/fluorescence microscopy. (a) Upright configuration. A high numerical aperture objective is positioned over the AFM probe. The resolution of the objective is 280 nm (water immersion) or 400 nm (in air). The upright configuration is optimized for AFM-Raman/fluorescence-SNOM imaging of opaque samples. (b) Inverted configuration. Optimized for use with transparent samples or nanometer-scale objects deposited on thin microscope glass. The objective lens from the bottom can have a resolution <200 nm (oil immersion). (c) Side illumination configuration. This setup is used for Tip-Enhanced Raman and fluorescence experiments.

NTEGRA Spectra

AFM + Confocal Raman + SNOM + TERS: Correlated Measurements on the Single Integrated System

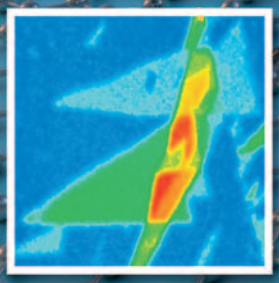

Raman: G-band intensity

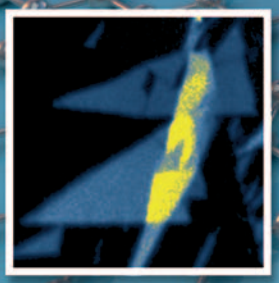

Raman: 2D band position

Rayleigh light intensity

AFM: Height

AFM: Lateral force

AFM: Force modulation

AFM: Kelvin probe

AFM: Electrostatic force

The same graphene flake imaged by different AFM and spectroscopy techniques in the single experiment

Search for the article "AFM + confocal Raman/Fluorescence + SNOM + Tip Enhanced Raman: equipment and applications" in this Microscopy Today issue.

www.ntmdt.com www.ntmdt-tips.com

NT-MDT
INTEGRATED SOLUTIONS FOR NANOTECHNOLOGY

Enter the Gift code at **www.ntmdt.com** and get a present from NT-MDT. Attention: limited quantity! Be in time to get your gift!

Enter code NTEGRA0601BI and get a gift*

Raman/fluorescence studies are required, the sample must be transparent or (for the case of small nanoparticles) should be deposited onto a transparent substrate. When opaque samples need to be studied, the upright configuration is used. In this configuration, high-resolution optics (100×, resolving power ≤400 nm) is positioned from the same side of the sample as the cantilever. Using special "elephant trunk-shaped" probes (produced by using standard Si cantilever technology) allows focusing of the laser light directly at the apex of the AFM tip.

In some special experiments, a side optical access to the AFM tip is essential (Figure 1c). This is realized by an additional objective lens to focus the laser light from the side of the AFM probe. Collection of the light from the sample can be accomplished with the same side objective or with the high-resolution objective from the top. The latter has the advantage of providing true confocal measurements with diffraction-limited resolution, which is not possible when the side objective is used for the light detection.

The optical AFM setup (in upright, inverted, or side illumination geometry) is connected to the confocal Raman module via a free-space optical coupling. Integrated AFM-Raman software allows control over AFM and Raman measurement parameters from one program. For correlated AFM and optical measurements, it is essential to position the AFM tip inside the laser spot with high precision. This is achieved by independent *XYZ*-scanning of the laser spot across the cantilever area or vice versa and recording the intensity of the Rayleigh scattered light or the Raman signal. Scanning is performed by closed-loop controlled piezos that ensure high positioning precision (at the nm scale) and high temporal stability.

After tip-to-laser-spot positioning, the sample is scanned. The AFM and Raman/fluorescence signals can be collected simultaneously (during one scan) providing spatially correlated physical and chemical information. During this one measurement, the AFM signals (such as height, cantilever's oscillation amplitude and phase, deflection and lateral force, electrical current, etc.) can be recorded simultaneously with hyperspectral (full spectrum at each point) Raman/fluorescence image from the same place on the sample. This provides spatially and temporally correlated AFM and spectral information from the sample. For some AFM modes, like magnetic force microscopy (MFM) [1, 3], a cantilever change is required. This procedure is done without losing the location on the sample to within <1 μm precision. The AFM-Raman software allows for further mathematical analysis and post-processing of hyperspectral and AFM images, their comparison, correlation, overlay, and so on. To ensure full flexibility for the research, the above-described measurements can be performed by all existing types of AFM/SPM probes: all types of contact and non-contact AFM cantilevers, Scanning Tunneling Microscopy (STM) tips in the tunneling regime, probes made from metal wires, and glass (or any other material) that is attached to the tuning fork (in normal force and shear force regimes). In addition, Scanning Near Field Optical Microscopy (SNOM) [1, 4, 5] probes of any type (quartz fibers, apertured Si cantilevers) can be used to provide SNOM laser and fluorescence imaging with resolution below the diffraction limit. Importantly, the measurements can be performed under environmental control: at variable humidity and temperature, in controlled atmosphere, in liquid, and even (in some configurations) in electrochemical environments.

Results

We have studied graphene on gold substrate using the combined AFM and Raman microscopy. The sample was placed in a controlled environment chamber, and measurements were done at low humidity (<20%). Figure 2b shows a bright field image of a graphene sample with the elephant-nose-shaped AFM cantilever fitted. The tightly focused

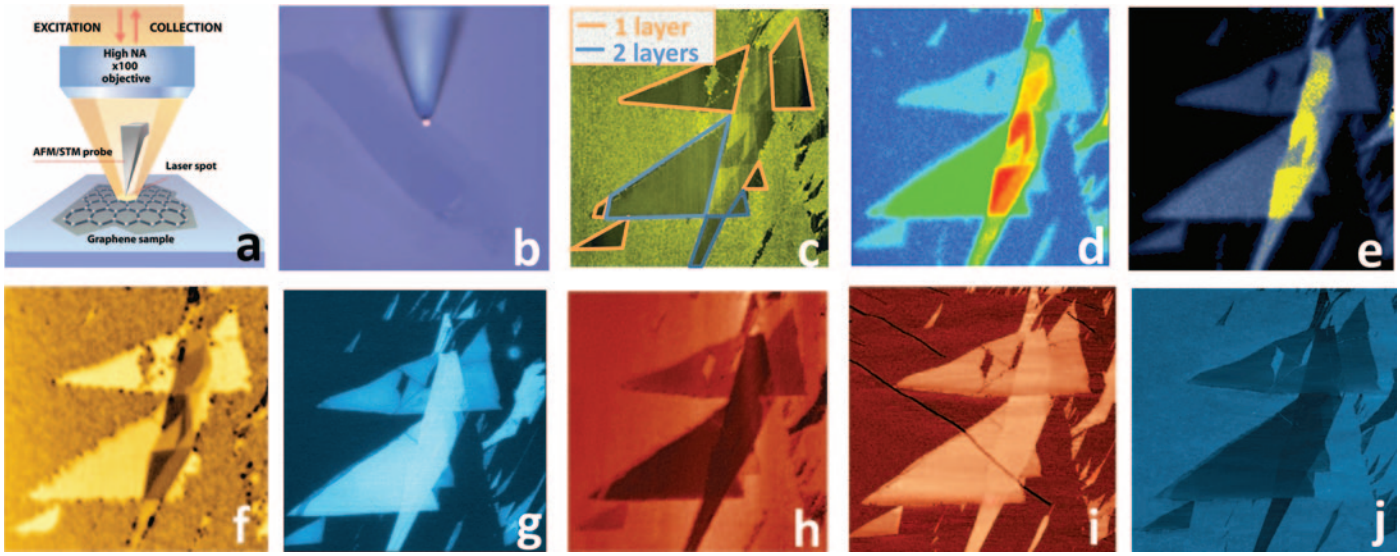

Figure 2: AFM-Raman/Rayleigh imaging of graphene on gold substrate. (a) Experimental configuration. (b) White light image of a graphene sample with AFM cantilever on the top and the laser spot focused precisely to the end of the AFM tip. (c) AFM topography of a graphene sample. Image scan: 30 × 30 μm. Regions with one, two, and more layers are observed as outlined by corresponding blue and orange lines. (d) Confocal Raman map, G-band intensity. (e) Confocal Raman map, center of mass of 2D (G') band. (f) Confocal image of Rayleigh (elastically scattered light). (g) Kelvin Probe Microscopy image (mapping surface potential, work function). (h) Electrostatic Force Microscopy image. (i) Force Modulation Microscopy image. (j) Lateral Force Microscopy image.

laser beam (the spot size ~400 nm) was positioned precisely (accuracy <10 nm) at the apex of the AFM cantilever using an automated alignment procedure. All measurements were performed in one experiment without removing the sample. Both hyperspectral Raman images and some of the AFM maps were obtained while the sample was scanned once. Cantilevers may be exchanged according to the AFM technique applied and reproducibly positioned with good precision (<1 μm) to the same sample area.

The sample thickness (number of graphene layers) in each region was measured by AFM and tracked proportionately by other methods. The AFM topography in Figure 2c gives a thickness of ~0.5–1 nm for each atomic layer of graphene. Regions with 1, 2, 3 and more layers are observed. Graphene flakes are atomically flat, whereas the gold substrate shows substantial roughness. The intensity of the G-band (~1580 cm^{-1}, corresponds to in-plane atom vibrations in crystal lattice) (Figure 2d), is approximately proportional to the number of layers. The second order D- (or, " 2D -" or " G'- ") Raman band shape and its center-of-mass position (Figure 2e) is also directly related to the number of layers in graphene [6–8]. Finally, the intensity of Rayleigh scattered light (Figure 2f) also provides a high positive as well as negative contrast (with respect to the substrate) depending on the number of layers.

Insight into graphene physical properties was provided by various advanced AFM techniques. Kelvin Probe Microscopy (SKM) [1, 9] measures the surface potential of the sample, and a clear contrast is observed in the SKM image (Figure 2g) between single-, double-, and triple- layer graphene flakes. The surface potential monotonically increases with the increasing number of layers. Localized surface charge is mapped by Electrostatic Force Microscopy (EFM) [1, 10] (Figure 2h); the EFM image shows strong contrast between single-, double-, and multiple-layer flakes. Force Modulation Microscopy [1, 11] (Figure 2i) measures the local elastic properties of the sample; a good contrast is seen between the softer gold substrate and the harder graphene sample and only a weak contrast between single- and multiple-layer flakes regions. Finally, Lateral Force Microscopy (LFM) [1, 12] is used to measure local friction between the Si cantilever and the sample. The LFM image (Figure 2j) shows that friction monotonically decreases with an increasing number of layers.

The ultimate goal of integrating AFM with Raman/fluorescence spectroscopy is to break the diffraction limit of light by using a special AFM probe and to reach optical resolution down to a few tens of nanometers. This can be achieved in the so-called Tip-Enhanced Raman/fluorescence (TERS microscopy experiment (Figure 3a) [13–22]. A special nano-antenna (an AFM probe of a certain chemical composition and shape) is placed at a specific point at the tightly focused laser spot (where the light polarization is most favorable) with <10 nm accuracy. Under specific physical conditions, the AFM nano-antenna can locally enhance the electromagnetic field intensity near the tip apex and become a localized "nano-source of light." The power density of the light can be locally increased by many orders of magnitude in the area within 10–50 nanometers of the tip end. A most common example of such nano-antennas is a metal tip (gold or silver) with a localized surface plasmon at the very tip having a frequency close to that of the incoming laser light. When scanning the sample with respect to such a nano-antenna, the obtained Raman/fluorescence map has a lateral resolution determined not by the laser spot size but by the size of electromagnetic field localization at the tip apex. The resolution of such TERS techniques can reach (with some samples) 10 nm [13].

Figure 3b shows a conventional confocal (micro) Raman map (G-band) of a single-walled carbon nanotube bundle with a 5-nm diameter (as measured by AFM). The bundle on the micro-Raman image has a ~250-nm thickness, which is determined by the diffraction-limited resolution of the confocal measurement (633-nm light, oil immersion optics with 1.4 NA). When a special TERS nano-antenna (a sharp gold tip in our case) is brought to the laser spot and kept a few nm away from the sample, the same Raman measurement (Figure 3c) provides a clearer picture. The measured width of the nanotube becomes ~50 nm, improving the resolution of the TERS technique in this "nano-Raman" experiment by a factor of 5 compared to diffraction-limited confocal microscopy.

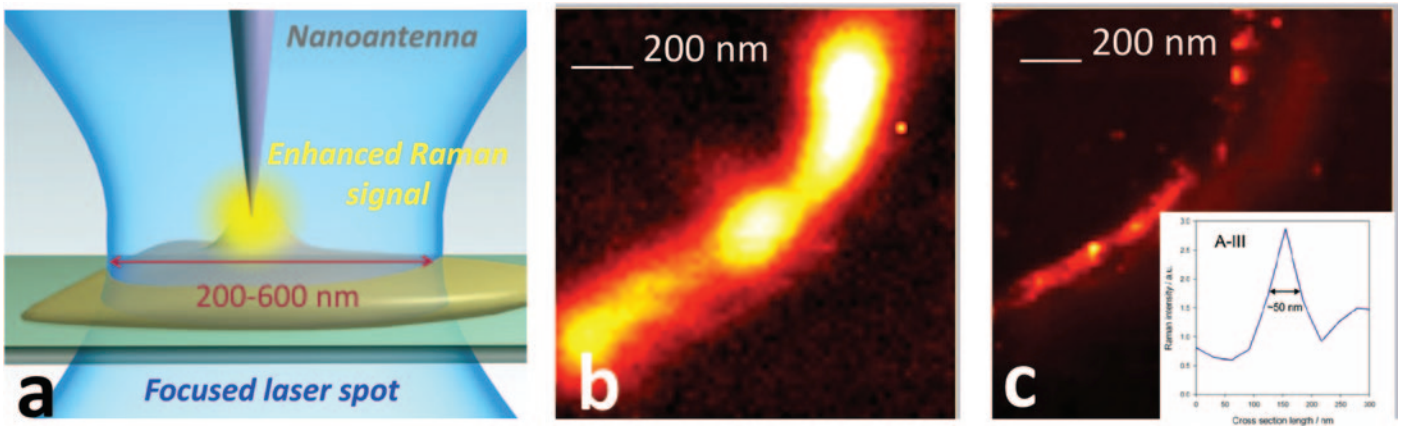

Figure 3: Tip-Enhanced Raman Spectroscopy (TERS) measurements of carbon nanotubes. (a) Schematic diagram showing the TERS principle. (b) Conventional micro-Raman map (G-band) of an individual carbon nanotube bundle (5-nm diameter). Resolution of the image is diffraction-limited to about 250 nm. (c) Nano-Raman (TERS) map of the same bundle with the special TERS tip in the laser focus kept a few nm over the sample. Resolution of the image is ~50 nm. It is not now limited by the wavelength of light but determined (roughly) by the size of the TERS tip.

Conclusion

In conclusion, we have demonstrated how integrated AFM–confocal Raman/fluorescence equipment provides extensive spatially correlated physical, chemical, and crystal structure information about the sample during one experiment. In order to break the diffraction limit of light optical resolution, special techniques can be applied such as SNOM and TERS.

References

[1] For an introduction to the AFM and overview of different AFM techniques, see http://www.ntmdt.com/page/primer.
[2] E Smith and G Dent, *Modern Raman Spectroscopy: A Practical Approach*, John Wiley and Sons Ltd., West Sussex, England, 2006.
[3] Y Martin, D Rugar, and HK Wickramasinghe, *Appl Phys Lett* 52(3) (1988) 244–48.
[4] DW Pohl, W Denk, and M Lanz, *Appl Phys Lett* 44 (1984) 651.
[5] U Diirig, D Pohl, and F Ronner, *J Appl Phys* 59 (1986) 3318–27.
[6] C Thomsen and S Reich, *Phys Rev Lett* 85 (2000) 5214.
[7] AV Baranov, AN Bekhterev, YS Bobovich, and VI Petrov, *Opt Spektrosk* 62 (1987) 1036.
[8] AC Ferrari, JC Meyer, V Scardaci, C Casiraghi, M Lazzeri, F Mauri, S Piscanec, D Jiang, KS Novoselov, S Roth, and AK Geim, *Phys Rev* 97 (2006) 187401.
[9] M Nonnenmacher, MP O'Boyle, and HK Wickramsasinghe, *Appl Phys Lett* 58 (1991) 2921.
[10] Y Martin, CC Williams, and HK Wickramasinghe, *J Appl Phys* 61 (1987) 4723.
[11] RD Young, US Pat. 5092163.
[12] CM Mate, GM McClelland, R Erlandsson, and S Chiang, *Phys Rev Lett* 59 (1987) 1942–45.
[13] RM Stöckle, YD Suh, V Deckert, and R Zenobi, *Chem Phys Lett* 318 (2000) 131.
[14] N Hayazawa, Y Inouye, Z Sekkat, and S Kawata, *Opt Commun* 183 (2000) 333.
[15] MS Anderson, *Appl Phys Lett* 76 (2000) 3130.
[16] MS Anderson and WT Pike, *Rev Sci Instrum* 73 (2002) 1198.
[17] WX Sun and ZX Shen, *J Raman Spectroscopy* 34 (2003) 668.
[18] Y Saito, M Motohashi, N Hayazawa, and S Kawata, *Appl Phys Lett* 88 (2006) 143109.
[19] N Hayazawa, M Motohashi, Y Saito, H Ishitobi, A Ono, T Ichimura, P Verma, and S Kawata, *J Raman Spectroscopy* 38 (2007) 684.
[20] D Mehtani, N Lee, RD Hartschuh, A Kisliuk, MD Foster, AP Sokolov, and JF Maguire, *J Raman Spectroscopy* 36 (2005) 1068.
[21] V Poborchii, T Tada, T Kanayama, and P Geshev, *J of Raman Spectroscopy* 40 (2009) 1377.
[22] SS Kharintsev, G Hoffmann, PS Dorozhkin, G de With, and J Loos, *Nanotechnology* 18 (2007) 315502.

MT